haematologica
Journal of the Ferrata Storti Foundation

A novel role of AURKA kinase in erythroblast enucleation

by Yuanlin Xu, Peijun Jia, Yating Li, Huan Zhang, Jingxin Zhang, Wanxin Li, Yazhe Zhen, Yan Li, Jiaming Cao, Tingting Zheng, Yihan Wang, Yanyan Liu, Xiuli An and Shijie Zhang

Received: Dec 16, 2023.
Accepted: June 7, 2024.

Citation: Yuanlin Xu, Peijun Jia, Yating Li, Huan Zhang, Jingxin Zhang, Wanxin Li, Yazhe Zhen, Yan Li, Jiaming Cao, Tingting Zheng, Yihan Wang, Yanyan Liu, Xiuli An and Shijie Zhang. A novel role of AURKA kinase in erythroblast enucleation. Haematologica. 2024 July 4. doi: 10.3324/haematol.2023.284873 [Epub ahead of print]

A novel role of AURKA kinase in erythroblast enucleation

Yuanlin Xu,[1,2*] Peijun Jia,[1*] Yating Li,[1*] Huan Zhang[1] Jingxin Zhang,[1] Wanxin Li,[1] Yazhe Zhen,[1] Yan Li,[1] Jiaming Cao,[1] Tingting Zheng,[1] Yihan Wang,[2] Yanyan Liu,[2] Xiuli An[3#] and Shijie Zhang[1#]

[1]School of Life Sciences, Zhengzhou University, Zhengzhou, China; [2]Department of Internal Medicine, The Affiliated Cancer Hospital of Zhengzhou University & Henan Cancer Hospital, Zhengzhou, China and [3]Laboratory of Membrane Biology, New York Blood Center, New York, NY, USA

XY, PJ and YL contributed equally as first authors.
#XA and SZ contributed equally as senior authors.

Correspondence: S. Zhang
shijie-zhang@zzu.edu.cn

X. An
xan@nybc.org

Received: December 16, 2023.
Accepted: June 7, 2024.
Early view: Xxxxxxxxxx.

https://doi.org/10.3324/haematol.2023.284873

Abstract

Generation of mammalian red blood cells requires the expulsion of polarized nuclei late in terminal erythroid differentiation. However, the mechanisms by which spherical erythroblasts determine the direction of nuclear polarization and maintain asymmetry during nuclear expulsion are poorly understood. Given the analogy of erythroblast enucleation to asymmetric cell division and the key role of Aurora kinases in mitosis, we sought to investigate the function of Aurora kinases in erythroblast enucleation. We found that AURKA (Aurora kinase A) is abundantly expressed in orthochromatic erythroblasts. Intriguingly, high-resolution confocal microscopy analyses revealed that AURKA co-localized with the centrosome on the side of the nucleus opposite its membrane contact point during polarization and subsequently translocated to the anterior end of the protrusive nucleus upon nuclear exit. Mechanistically, AURKA regulated centrosome maturation and localization via interaction with γ-tubulin to provide polarization orientation for the nucleus. Furthermore, we identified ECT2 (epithelial cell transforming 2), a guanine nucleotide exchange factor, as a new interacting protein and ubiquitination substrate of AURKA. After forming the nuclear protrusion, AURKA translocated to the anterior end of the protrusive nucleus to directly degrade ECT2, which is partly dependent on kinase activity of AURKA. Moreover, knockdown of ECT2 rescued impaired enucleation caused by AURKA inhibition. Our findings have uncovered a previously unrecognized role of Aurora kinases in the establishment of nuclear polarization and eventual nuclear extrusion and provide new mechanistic insights into erythroblast enucleation.

Introduction

Enucleated red blood cells are produced by the multistage process of erythropoiesis that begins with hematopoietic stem and progenitor cells to committed lineage-restricted erythroid progenitors followed by four to five mitoses to differentiate sequentially into proerythroblasts, basophilic erythroblasts, polychromatic erythroblasts, orthochromatic erythroblasts. During the late stage of terminal erythroid differentiation, orthochromatic erythroblasts exit the cell cycle and expel their nuclei to give rise to enucleated reticulocytes.[1] Preceded by proper nuclear condensation that required histone deacetylation,[2-4] the condensed nucleus moves and polarizes to one side of the orthochromatic erythroblast. Nuclear polarization, which is generally considered the outset of enucleation, requires microtubules and microtubule-dependent local activation of phosphoinositide 3-kinase.[5] Subsequently, a contractile actomyosin ring is formed between the nascent reticulocyte and extruding nucleus (pyrenocyte) mediated by Rac GTPases and their downstream effectors.[6-8] In addition, vesicle trafficking has been shown to play an important role in driving enucleation.[9,10] Despite these studies, the molecular mechanisms of how the spherical erythroblasts determine the direction of nuclear polarization and accomplish the final separation of the nucleus from the nascent reticulocytes remain largely unclear.

Aurora kinases are highly conserved serine/threonine kinases required for regulation of mitosis (AURKA and AURKB) and meiosis (AURKC). During mitosis progression, AURKA plays an essential role in controlling centrosome maturation and separation, two events representing the earliest stages of mitotic spindle formation. In contrast, AURKB mainly regulates chromosome condensation, spindle assembly checkpoint, and final cytokinesis by providing catalytic activity to the heterotetrameric chromosome passenger

complex.[11-14] Inactivation of AURKA leads to monopolar spindles and chromosomal separation defects, ultimately leading to mitotic arrest and cell apoptosis,[15,16] whereas inactivation of AURKB results in final failure cytokinesis due to abnormal chromosome alignment, kinetochore-microtubule attachment, and cleavage furrow formation.[17,18] Due to indispensable functions in cell division and overexpression in multiple cancers, Aurora kinases have attracted great interest in cell and cancer biology at present. Multiple functions in mitosis and non-mitotic biological processes are uncovered.[11,15-19] However, up to now, the role of Aurora kinases in erythroid cells, especially in erythroblast enucleation has been investigated.

More notably, Aurora kinases are generally expressed at high levels in rapidly dividing cells and tissues, such as embryonic cells, hematopoietic cells, and cancer cells.[15-18] Conversely, the expression of Aurora kinases is low or absent in most adult tissues or cells due to their lower proliferation rates. Here we found surprisingly that AURKA is highly expressed in the non-dividing orthochromatic erythroblasts, suggesting a novel role of AURKA in erythroblast enucleation. Using pharmacologic and genetic approaches in conjunction with high-resolution confocal microscopy, we documented that Aurora kinase A plays a critical role in nuclear polarization and enucleation via regulation of centrosome localization and ECT2 degradation.

Methods

Antibodies and reagents

The antibodies utilized for western blotting, flow cytometric analysis and immunofluorescence in this study can be found in *Online Supplementary Table S1*. Inhibitors Alisertub (MLN8237), were purchased from Selleck. Inhibitor Centrinone was purchased from MedChem Express. Dimethyl sulfoxide (DMSO) was used to dissolve MLN8237 or Centrinone, and the same DMSO vehicle was employed in the control condition (0 μM) to ensure consistency.

CD34$^+$ cells culture

Primary human CD34$^+$ cells were isolated through magnetic beads (Miltenyi Biotechnology, Bergisch Gladbach, Germany). These CD34$^+$ cells were then induced towards the erythroid lineage utilizing a three-phase culture system. The cell culture details have been described previously.[1]

Flowcytometry analysis

Enucleation was assessed by staining with the nucleic acid dye Hoechst33342 for 15 minutes in phosphate-buffered saline (PBS) with 2% fetal bovine serum (FBS). Cell cycle analysis was performed by staining DNA using 50 mg/mL propidium iodide (Sigma-Aldrich) following permeabilization in 100 mL of 0.1% Triton X-100. Data analysis was performed using the Flow Jo software package.

Orthochromatic erythroblasts sorting

Cells obtained from tibia and femur of mice were suspended in PBS/2 mM EDTA/2% FBS buffer. Mouse bone marrow orthochromatic erythroblasts were sorted using a FACS Aria II cell sorter (BD Biosciences, USA). Sorted cells were cultured for 18 hours and then used for staining and flow analysis.

Immunofluorescence

Immunofluorescence was carried out according to the protocol previously described.[8] Cells were fixed in 4% paraformaldehyde for 6 hours and blocked with 5% goat serum in PBS with 0.1% Triton-X 100 for 15 minutes at room temperature. The cells were subsequently incubated with primary antibodies against AURKA (1:500) antibody, γ-tubulin (1:1000), α-tubulin (1:500) and ECT2 (1:500) at 4°C overnight. Secondary antibodies, Cy3-conjugated goat anti-rabbit IgG secondary or FITC-conjugated mouse anti-IgG (1:100, Boster Biological Technology), were applied for 2 hours at 37°C. Labeled cells were counterstained with 4',6-diamidino-2-phenylindole (DAPI; #D8417; 1:1,000, Sigma-Aldrich).

Small interfering RNA transfection

AURKA and *ECT2* small interfering RNA (siRNA) as well as control scramble siRNA, were transfected into erythroblasts on day 15 of culture according to the manufacturer's protocol (RIB&BIO, China). For detailed sequence information, refer to *Online Supplementary Table S3*.

Cytospin preparation

Cytospins were prepared by centrifuging 1×10^5 cells in 200 μL PBS for 10 minutes at 280 rpm onto glass slides using a Cytospin 4 apparatus (Thermo, Germany). The slides were then fixed with methanol for 3 minutes, and then directly stained with a diluted Gimesa reagent (Solarbio, China) at room temperature for 10-15 minutes. Cells were imaged using an Olympus IX73 microscope.

Western blotting

Western blotting analysis was performed following previously published procedures.[20] In order to determine protein expression levels, Image J software was utilized for quantification.

Approval for the use of human and mouse cells

All studies using anonymized primary human and mouse cells were conducted in accordance with applicable laws and approved by the Institutional Review Board of Zhengzhou University (approval number ZZUIRB2023-243).

Statistics

All experiments were replicated at least three times. The data was analyzed using GraphPad Prism 8.0 software. *P* values were determined by either one-way ANOVA (with Bonferroni's *post hoc* test) or *t* tests. For all data, $P<0.05$ was considered to indicate a statistically significant difference;

*P<0.05, **P<0.01, ***P<0.001. Data are expressed as mean ± standard deviation.

Results

Aurora A expression was upregulated in late-stage erythroblasts

As a first step to investigate the role of Aurora kinases in erythropoiesis, we examined their expression during human terminal erythroid differentiation. Figure 1A shows our RNA-sequencing data of erythroblasts cultured from cord blood CD34$^+$ cells at distinct stages of development,[20] which reveals abundant expression of *AURKA* and *AURKB* with distinct expression patterns, with *AURKA* upregulated while *AURKB* downregulated in late-stage erythroblasts. No *AURKC* mRNA transcripts were detected in erythroblasts (*data not shown*). The expression patterns of Aurora kinases were further confirmed by quantitative real time polymerase chain reaction (qRT-PCR) analysis (Figure 1B) and western

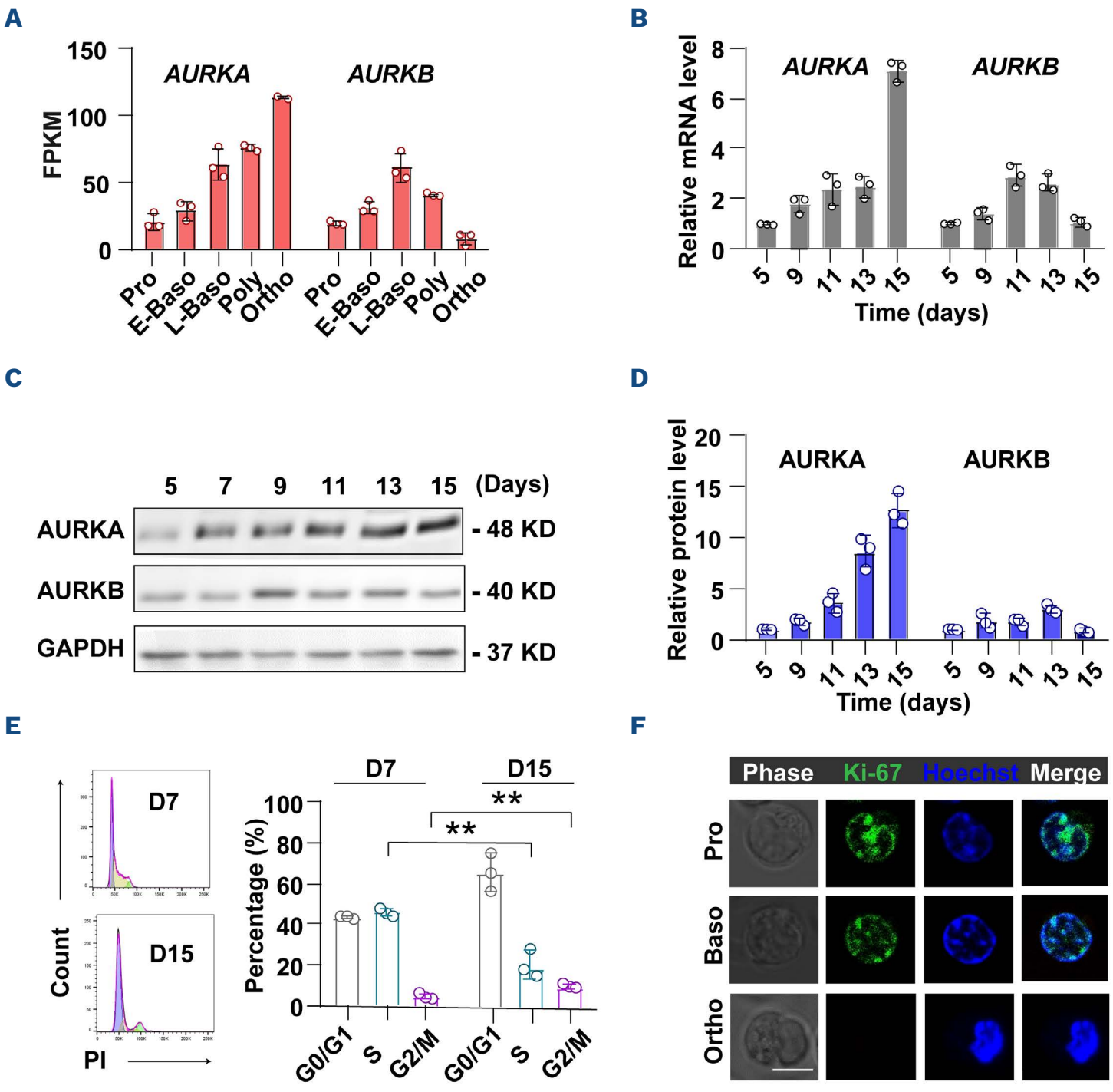

Figure 1. Expression of Aurora kinases during terminal erythroid differentiation. (A) RNA-sequencing data revealed the gene expression levels of *AURKA* (Aurora kinase A) and *AURKB* (Aurora kinase B) at distinct stages of human terminal erythroid differentiation, including proerythroblasts (Pro), early basophilic erythroblasts (E-Baso), late basophilic erythroblasts (L-Baso), polychromatic erythroblasts (Poly), and orthochromatic erythroblasts (Ortho). (B) Quantitative real time polymerase chain recation was employed to assess the mRNA expression levels of *AURKA* and *AURKB* in cultured erythroblasts at 5, 9, 11, 13, and 15 days. (C) Western blotting images showed the protein levels of AURKA and AURKB in cultured erythroblasts from day 5 to 15. (D) Quantitative analysis of protein levels was performed on erythroblasts cultured for indicated days. (E) Representative flow cytometry profiles showed the cell cycle progression of erythroblasts cultured for 7 and 15 days. The percentages of erythroblasts in each phase of the cell cycle on day 7 and day 15 were determined under the specified conditions using propidium iodide (PI) staining. (F) Immunofluorescence images exhibited the cellular expression of Ki-67 (green) in Pro, Baso, and Ortho erythroblasts, sorted from 3 independent biological replicates. Hoechst33342 (blue) was used to stain the nucleus. Scale bar =5 μm; **P<0.01.

blotting analysis (Figure 1C, D). Given that late-stage terminal erythroblasts gradually exit the cell cycle prior to enucleation (Figure 1E), and orthochromatic erythroblasts can no longer divide as evidenced by undetectable Ki67$^+$ signal in orthochromatic erythroblasts (Figure 1F), the abundant expression of AURKA and its upregulation in late-stage erythroblasts is striking because AURKA is usually involved in the regulation of mitosis progression and is not expressed in cells that no longer divide.[11] Our finding suggests a novel role (non-mitosis-related role) of AURKA in erythroblast enucleation.

Inactivation of AURKA inhibited erythroblast enucleation

In order to examine whether AURKA plays a role in erythroblast enucleation, we first tested whether pharmacological inhibition of AURKA affects the enucleation of human erythroblasts. To this end, we differentiated cord blood CD34$^+$ cells into erythroid cells using our three-phase erythroid culture system.[1] The cells on day 15, most of which were orthochromatic erythroblasts, were then treated with MLN8237 (Aliseritib, AURKA-selective inhibitor) and enucleation rate was assessed after 48 hours of culture (*Online Supplementary Figure S1A*). Hoechest33342 staining revealed a representative enucleation profile, and quantitative analysis demonstrated that treatment of erythroblasts with MLN8237 inhibited enucleation (Figure 2A). Similar results were obtained using sorted mouse bone marrow orthochromatic erythroblasts (*Online Supplementary Figure S1B, C*). We attempted to use shRNA-mediated knockdown and CRISPR-mediated knockout approaches to examine the effect of AURKA. Unfortunately, cells could not differentiate into terminal erythroblasts due to severe apoptosis, indicating the critical role of AURKA in early-stage erythropoiesis, likely as a mitosis regulator. Instead, we carried out a siRNA-mediated knockdown approach. For this, the erythroblasts on day 13 of culture were transfected with *AURKA* siRNA and enucleation was assessed 48 hours later (*Online Supplementary Figure S1D*). *AURKA* was efficiently downregulated by all the three siRNA Oligos used as demonstrated by qRT-PCR and western blot (Figure 2B; *Online Supplementary Figure S1E*). Figure 2C shows that knockdown of AURKA inhibited enucleation.

Inactivation of AURKA inhibited nuclear polarization in a microtubule-independent manner

Nuclear polarization is considered as the prerequisite of erythroblast enucleation.[21] We next examined whether AURKA regulates nuclear polarization by measuring the Δcentroid distribution (distance between centers of the cytoplasm and nucleus) (Figure 2D). Figure 2E shows that the mean Δcentroid was significantly reduced in MLN8237-treated erythroblasts. However, the size of the nucleus and cells remained unchanged in MLN8237-treated erythroblasts (*Online Supplementary Figure S1F*). Representative cytospin images support the flow cytometry results, clearly illustrating a broader field of view that allows a clearer assessment of enucleation and polarization differences between *AURKA* siRNA and scramble (*Online Supplementary Figure S1G, H*). Previous studies demonstrated that microtubule organization is required for proper polarization of nucleus during enucleation.[5,7] We therefore asked whether AURKA inactivation-mediated impaired polarization impairment is associated with microtubules. In order to address this, we examined the relationship between microtubule structure and nuclear positioning during enucleation using immunofluorescence. As expected, MLN8237 treatment resulted in disordered microtubule organization in erythroid cells undergoing mitosis, while interestingly, MLN8237 had no effect on microtubule organization in polarized erythroblasts (Figure 2F), suggesting that AURKA regulates nuclear polarization in a microtubule-independent manner.

Dynamic changes of AURKA localization during erythroblast enucleation

AURKA is a highly conserved serine/threonine kinase, which is associated with centrosome maturation and biopolar spindle assembly during mitosis and cytokinesis.[11,13,14] Although erythroblast enucleation is proposed to be analogous to asymmetric cell division, the localization of AURKA during enucleation has not been characterized to date. Therefore, we first detected AURKA location in human erythroblasts using high-resolution confocal microscopy. While AURKA was diffusely distributed throughout the cytoplasm of non-polarized erythroblasts (Figure 3Ai), it was localized at the posterior end of the nucleus (membrane contact point is considered the anterior end) in polarized erythroblasts (Figure 3Aii). Interestingly, in the enucleating erythroblasts, it translocated to the anterior end of the protrusive nucleus (Figure 3Aiii, B, C). When the nucleus was completely expulsed from the cytoplasm, AURKA was again dispersed throughout the cytoplasm. Similar changes in AURKA location were observed during mouse erythroblast enucleation (*Online Supplementary Figure S2*).

Given the relationship between AURKA and centrosome maturation in mitosis and similar foci positioning, we asked whether AURKA colocalizes with γ-tubulin in interphase centrosomes throughout erythroid differentiation and enucleation. In line with previous reports,[5-8] AURKA co-localized with γ-tubulin in centrosomes during cytokinesis in early erythroblasts (Figure 3D). However, while the distribution of AURKA followed the pattern of “dispersed-foci at the rear of nucleus-foci translocated to anterior end of nucleus” on enucleation progress, the bright spot of cytoplasmic γ-tubulin remained at the rear of the nucleus and traveled with the nucleus throughout expulsion until the nucleus was ready to separate (Figure 3D). The distance between AURKA and centrosome was obviously longer in the enucleating cell than in the polarized cell (Figure 3E). Figure 3F shows the statistical analysis of the percentage of co-localization of AURKA and centrosome in non-polarized cells, polarized cells, and enucleated cells. That is, AURKA co-localized with

the centrosome during polarization and subsequently solely translocated to the anterior end of the protrusive nucleus upon nuclear exit. These observations suggest that AURKA may provide direction for nucleus polarization by controlling centrosome maturation, but performs a centrosome-independent function during subsequent nucleus expulsion.

AURKA controls nuclear polarization by regulating centrosome maturation

Co-localization of AURKA and centrosome during nuclear polarization raised the question whether AURKA controls polarization by regulating centrosome organization and maturation. Co-immunoprecipitation (co-IP) verified a direct interaction between AURKA and γ-tubulin (*Online Supplementary Figure S3A*). We then examined whether inhibition of AURKA altered the expression levels of γ-tubulin. The human erythroid cell line K562, being in the stage of pluripotent myeloid progenitor cell, provides a model system for studying erythroid differentiation and eukaryotic gene regulation due to its response to hemin and compounds.[22,23] Uninduced cells were used to simulate rapidly dividing cells, while cells on day 4 after hemin induction were mainly in

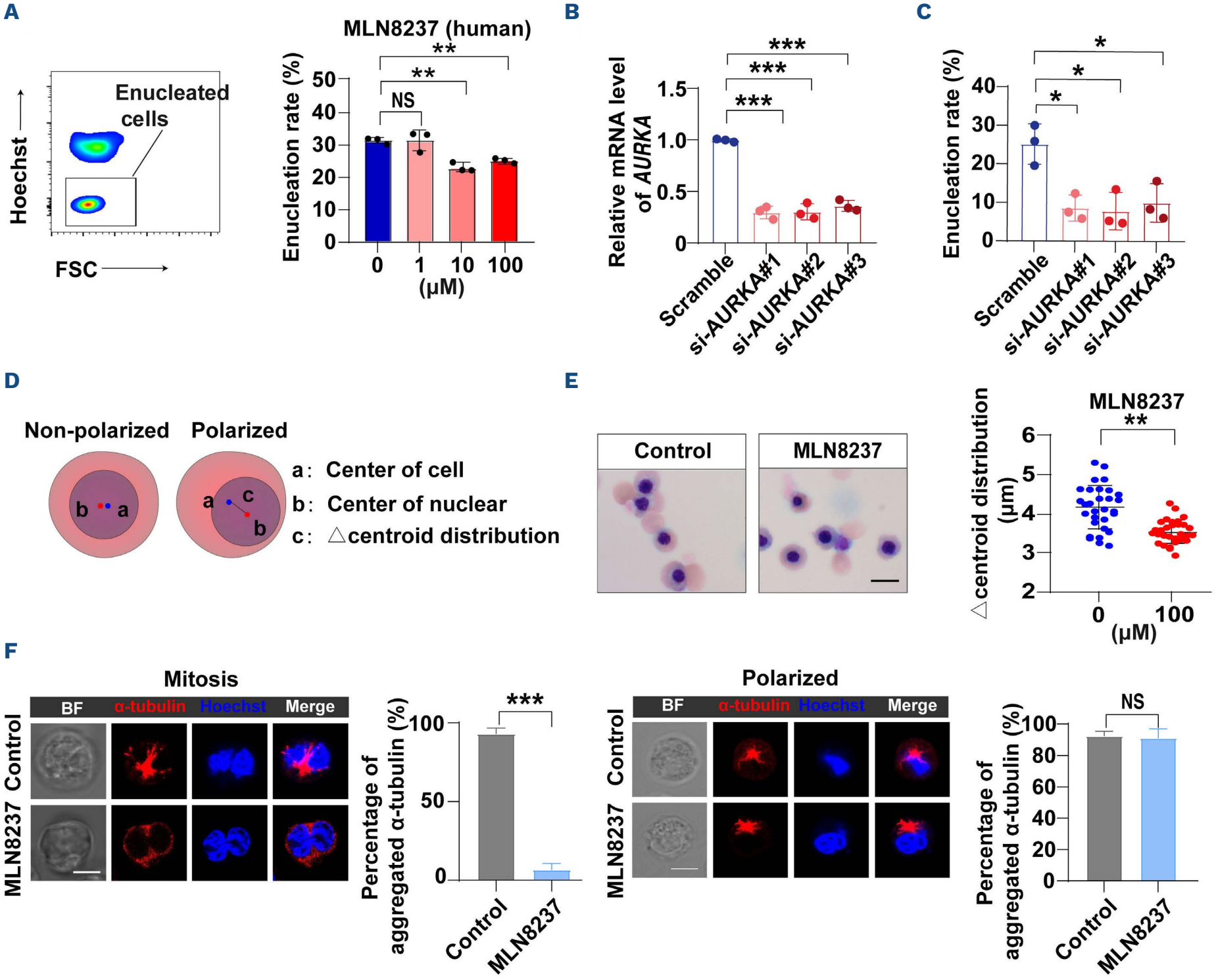

Figure 2. Inactivation of Aurora kinases blocks erythroblast enucleation. (A) Enucleation was assessed in the presence or absence of MLN8237 for cultured erythroblasts. (B) Quantitative analysis of the knockdown efficiency of small interfering RNA *AURKA* (siRNA-AURKA). (C) Quantitative analysis of the enucleation rates of siRNA-AURKA. (D) Schematic of polarized distance by measuring the Δcentroid distribution (c) from cell center (a) to nuclear center (b). (E) Representative cytospin images showed enucleation after treated with or without MLN8237 for 48 hours. Scale bar =10 μm. Quantitative analysis of the mean Δcentroid revealed a significant reduction in erythroblasts treated with MLN8237 after incubation for 48 hours. (F) Confocal microscopy showed MLN8237-induced microtubule disorganization during early erythroblast mitosis, with statistical α-tubulin aggregation analysis. MLN8237 treatment had no effect on microtubule organization during polarized orthochromatic erythroblasts, as observed in confocal microscopy images, also supported by statistical α-tubulin aggregation analysis. Scale bar =5 μm; **P*<0.05, ***P*<0.01, ****P*<0.001; NS: not significant.

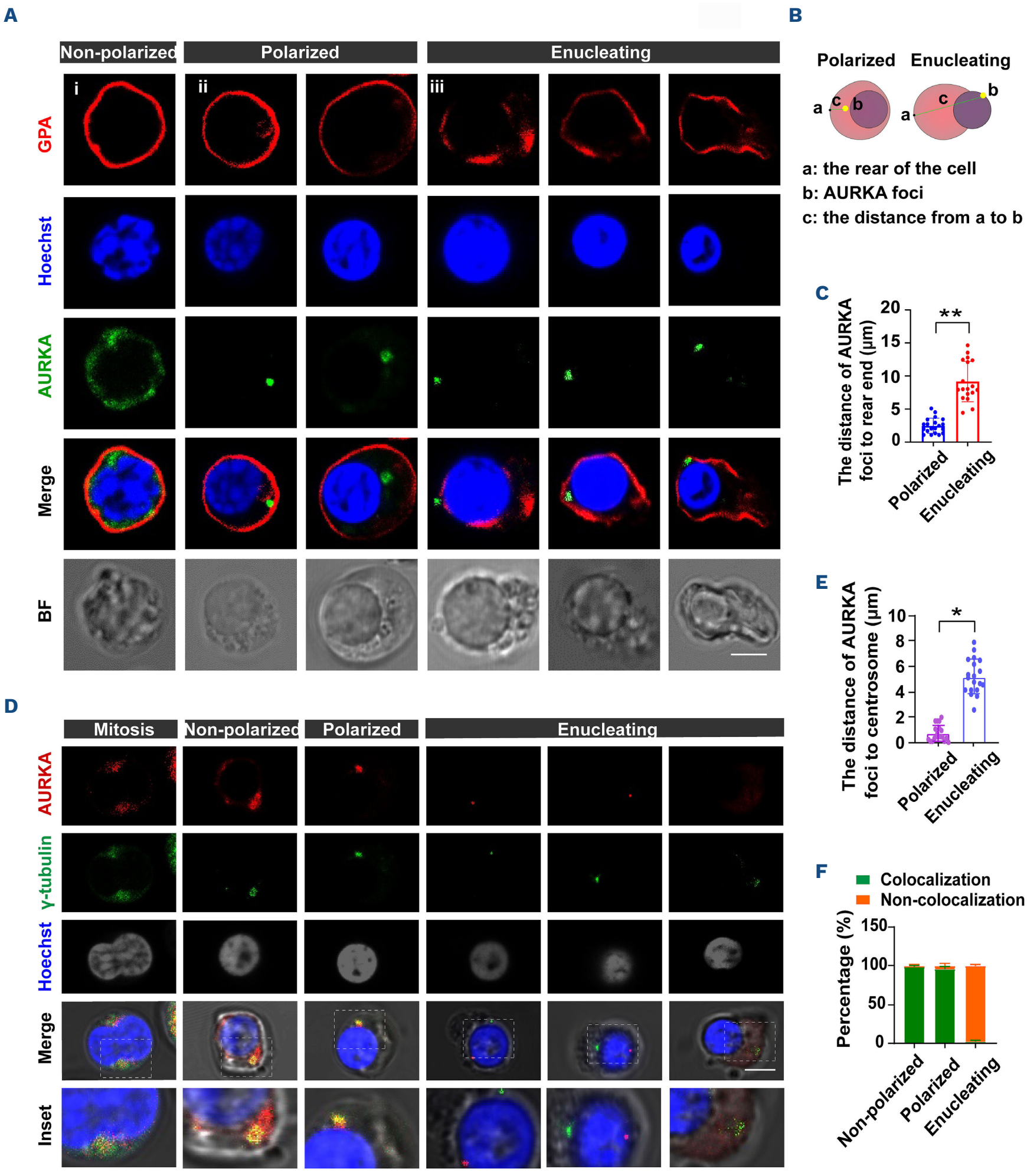

Figure 3. The localization of AURKA during erythroblast enucleation. (A) Confocal microscope images showed the location of AURKA proteins (green) at various stages of enucleation. GPA (red) was used to stain the membrane of terminal erythroid cells. Hoechst33342 (blue) was used to stain the nucleus. (B) Schematic of AURKA foci moving trail (c) by measuring the distance from AURKA foci (a) and the farthest end of the cell (b). (C) Quantification of distance traveled by AURKA foci in non-polarized cells, polarized cells and enucleating cells. (D) Confocal microscope images showed colocalization of AURKA (red) and centrosome (stain by γ-tubulin, green) in non-polarized cells, polarized cells and enucleating cells. (E) Quantification of distance from AURKA foci to centrosomes in non-polarized cells, polarized cells and enucleating cells. (F) Quantification of distribution of co-localization of AURKA and centrosome in non-polarized cells, polarized cells and enucleating cells. Scale bar =5 μm; *P<0.05, **P<0.01.

the late stage of erythroid terminal differentiation. Here, untreated K562 cells and cells induced for erythroid differentiation and maturation with hemin for 48 hours were incubated with MLN8237 respectively. After another 48 hours, total RNA and proteins were collected. Western blotting analysis showed that AURKA inhibitor did not alter the expression levels of γ-tubulin in both hemin-induced and non-induced groups (*Online Supplementary Figure S3B, C*), indicating that the interaction between AURKA and γ-tubulin is not responsible for protein expression of γ-tubulin. However, immunofluorescence showed that MLN8237 treatment obviously impaired the proper organization of centrosome (Figure 4A-C). Unlike the abiding foci positioning in control erythroblasts during enucleation, γ-tubulin proteins are diffusely distributed throughout the cytoplasm of non-polarized erythroblasts, polarized erythroblasts, and enucleating erythroblasts in MLN8237-treated cells (Figure 4A-C). Figure 4D presents the statistical analysis of the percentage of co-localization between AURKA and the centrosome in non-polarized cells, polarized cells, and enucleated cells before and after MLN8237 treatment. The dispersion of the centrosome was also observed when *AURKA* siRNA was utilized (*Online Supplementary Figure S3D-F*). It indicated that inhibition of AURKA significantly disrupts centrosome organization and maturation.

In order to directly test the role of centrosomes during

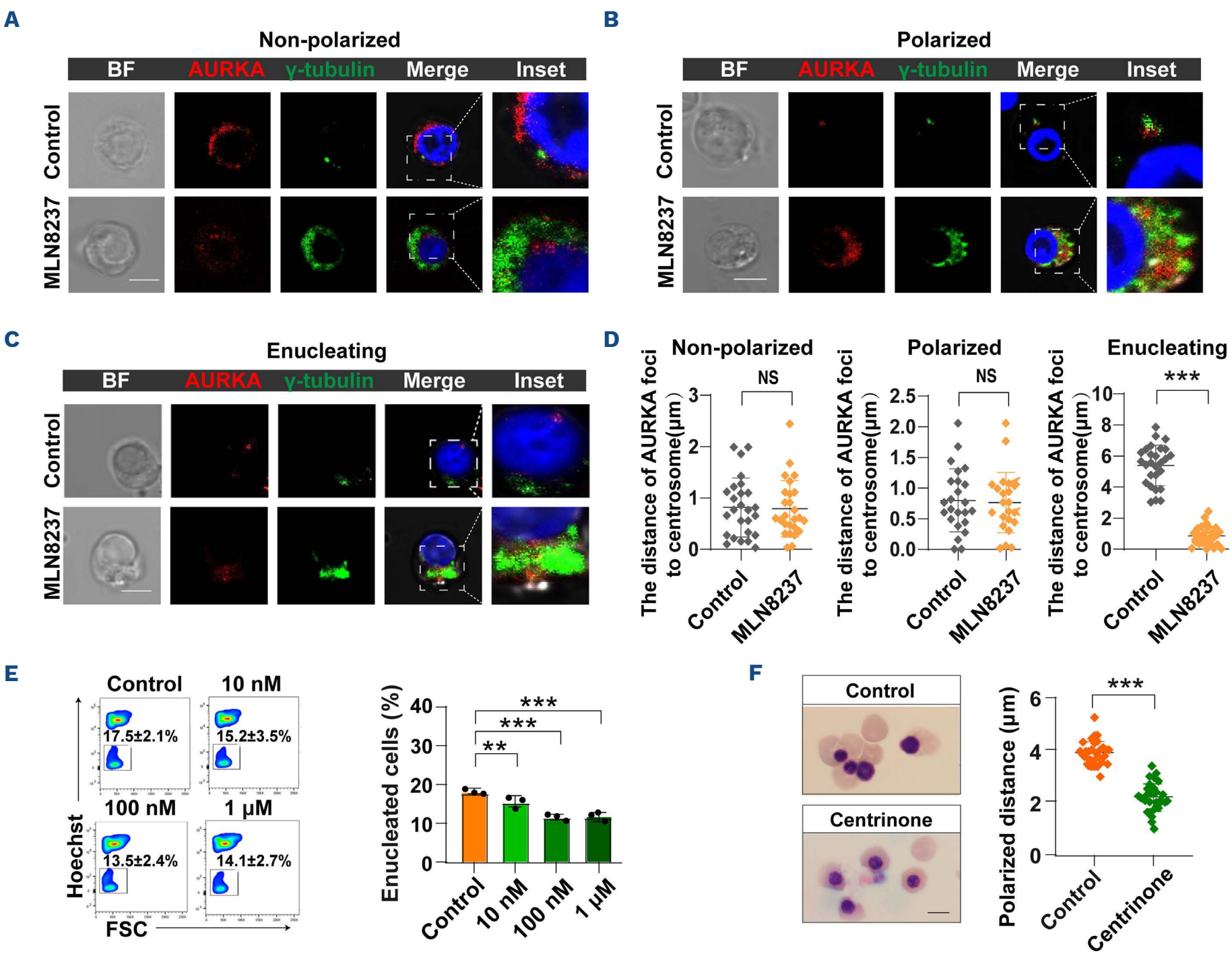

Figure 4. AURKA controls nuclear polarization by regulating centrosome maturation. Confocal microscope images showed the co-localization of AURKA and γ-tubulin in non-polarized cells (A), polarized cells (B) and enucleating cells (C) treated with or without MLN8237 for 48 hours. Scale bar =5 μm. (D) Quantification of distance from AURKA foci to centrosomes in (A), (B) and (C). (E) Representative flow cytometric analysis plot of the enucleation efficiency of centrinone-treated erythroblasts at the indicated concentrations. Statistical analysis depicted the enucleation efficiency of day 15 erythroblasts treated with or without centrinone for 48 hours. (F) Representative cytospin images in erythroblasts cultured with or without centrinone (100 nM). Quantification of polarized distance in orthochromatic erythroblasts treated with or without centrinone. Scale bar =10 μm; NS: not significant; ***P*<0.01, ****P*<0.001

erythroblast enucleation, we depleted centrosomes during enucleation using centrinone-B, an inhibitor of the master centriole biogenesis regulator PLK4, to treat CD34$^+$ cell-derived human erythroblasts at day 15 for 48 hours, due to previous reports that multiple cell divisions were needed to complete deplete of centrosomes.[24,25] Hoechst33342 staining showed that centrinone-B treatment significantly reduced the rate of enucleation in a dose-dependent manner (Figure 4E). Likewise, Δcentroid distribution showed impaired polarization of centrinone-B-treated erythroblasts (Figure 4F). These phenotypes mimic the results of AUKRA-deficient erythroblasts, suggesting a close connection between AUKRA and centrosome in polarization during erythroblast enucleation.

AURKA regulates the expression and localization of ECT2 during enucleation

Having identified AURKA's role in polarization and established the uncoupled centrosome localization pattern during nucleus expulsion, we next sought to answer why AURKA translocated to the anterior end of the protruding nucleus upon nuclear exit. We hypothesized that the movement of AURKA may be intended to alter the distribution of proteins associated with the establishment and maintenance of cell asymmetry to facilitate the final separation of pyrenocytes from nascent reticulocytes. The Rho subfamily of small GTPases, including Rac1/2, RhoA and Cdc42, has been shown to be essential for terminal erythroblast maturation and enucleation.[6,8,26,27] During embryonic development, the asymmetric distribution of ECT2, a guanine nucleotide exchange factor, is important for translocation of PAR proteins and Rho small GTPases to the precortex to maintain the established anterior-cortical domains.[28] Therefore, we examined whether AURKA involved in ECT2 expression and localization during enucleation. We found that ECT2 was diffusely distributed throughout the cytoplasm of non-polarized and polarized erythroblasts, but constricted at the rear of the translocating nucleus in enucleating erythroblasts, as observed through confocal microscopy (Figure 5A, B). We utilized Image Stream analysis to enhance our understanding of the localization of AURKA and ECT2 in polarized and enucleating cells. The fluorescence images and quantitative assessments revealed that AURKA was positioned at the posterior end of the nucleus in polarized erythroblasts. Interestingly, in enucleating erythroblasts, it underwent translocation to the anterior end of the protrusive nucleus (*Online Supplementary Figure S4A, B*). Additionally, we confirmed that ECT2 was diffusely distributed throughout the cytoplasm of polarized erythroblasts (*Online Supplementary Figure S4A*). However, in enucleating erythroblasts, ECT2 was observed to be constricted at the rear of the translocating nucleus (*Online Supplementary Figure S4B*). The statistical analysis also corroborated this trend (*Online Supplementary Figure S4C, D*).

Inhibition of AURKA impaired translocation of ECT2. Similar results were obtained using mouse bone marrow erythroblasts (*Online Supplementary Figure S5A-C*). Interestingly, this pattern of ECT2 localization was not observed during cytokinesis as demonstrated by the diffuse ECT2 expression in the cytoplasm of mitotic erythroid cells, and lack of effect of the AURKA inhibitor on ECT2 distribution (Figure 5B), indicating that AURKA regulation of ECT2 localization is restricted to enucleation.

In order to gain mechanistic insight into AURKA regulating ECT2, we first checked the expression pattern of ECT2 during erythropoiesis. RNA-sequencing data of erythroblasts cultured from cord blood CD34$^+$ cells at distinct stages of development[20] showed that the expression of *ECT2* was dramatically downregulated in orthochromatic erythroblasts (Figure 5C). The expression pattern of ECT2 at protein level was further confirmed by western blotting analysis (Figure 5D). We then examined the effects of AURKA inhibition on the expression of ECT2 in terminal erythroid cells. Western blotting analysis revealed that MLN8237 treatment resulted in a significant increase of ECT2 proteins in hemin-induced K562 cells on day 4. In contrast, there was no change in ECT2 expression in K562 cells that were not hemin-induced (Figure 5E, F), suggesting the specific function of AURKA on ECT2 expression during terminal erythroblast maturation.

In order to examine the impact of ECT2 overexpression on the process of enucleation, we constructed ECT2 overexpression vectors and transfected them into CD34$^+$ cells to induce erythroid differentiation (*Online Supplementary Figure S6A*). Our findings revealed that ECT2 overexpression had minimal influence on erythroid differentiation (*Online Supplementary Figure S6B, C*). However, it significantly impeded the process of enucleation (*Online Supplementary Figure S6D-F*). This indicates that AURKA might be impacting enucleation through ECT2.

AURKA promotes ubiquitin-mediated ECT2 degradation

The antagonistic localizations and expression levels led us to speculate that AURKA may have the function of degrading ECT2. Previous studies have reported that the ECT2 protein may be degraded through the ubiquitin-proteasome pathway.[29,30] Furthermore, AURKA, in addition to its kinase activity, has been predicted to possess ubiquitination activity.[31,32] However, it is unclear whether AURKA regulates ECT2 ubiquitination and degradation. To address this, we first performed a co-IP assay and found the direct interaction between AURKA and ECT2 (Figure 6A). Furthermore, when the effects of AURKA on the ubiquitin modification of ECT2 in cells were evaluated, the results showed that AURKA overexpression promoted ubiquitination of ECT2 (Figure 6C). We next examined the relationship between AURKA kinase activity and ECT2 degradation. The kinase activity of human AURKA is regulated by phosphorylation of threonine 288 (Thr 288) and mutations in this residue

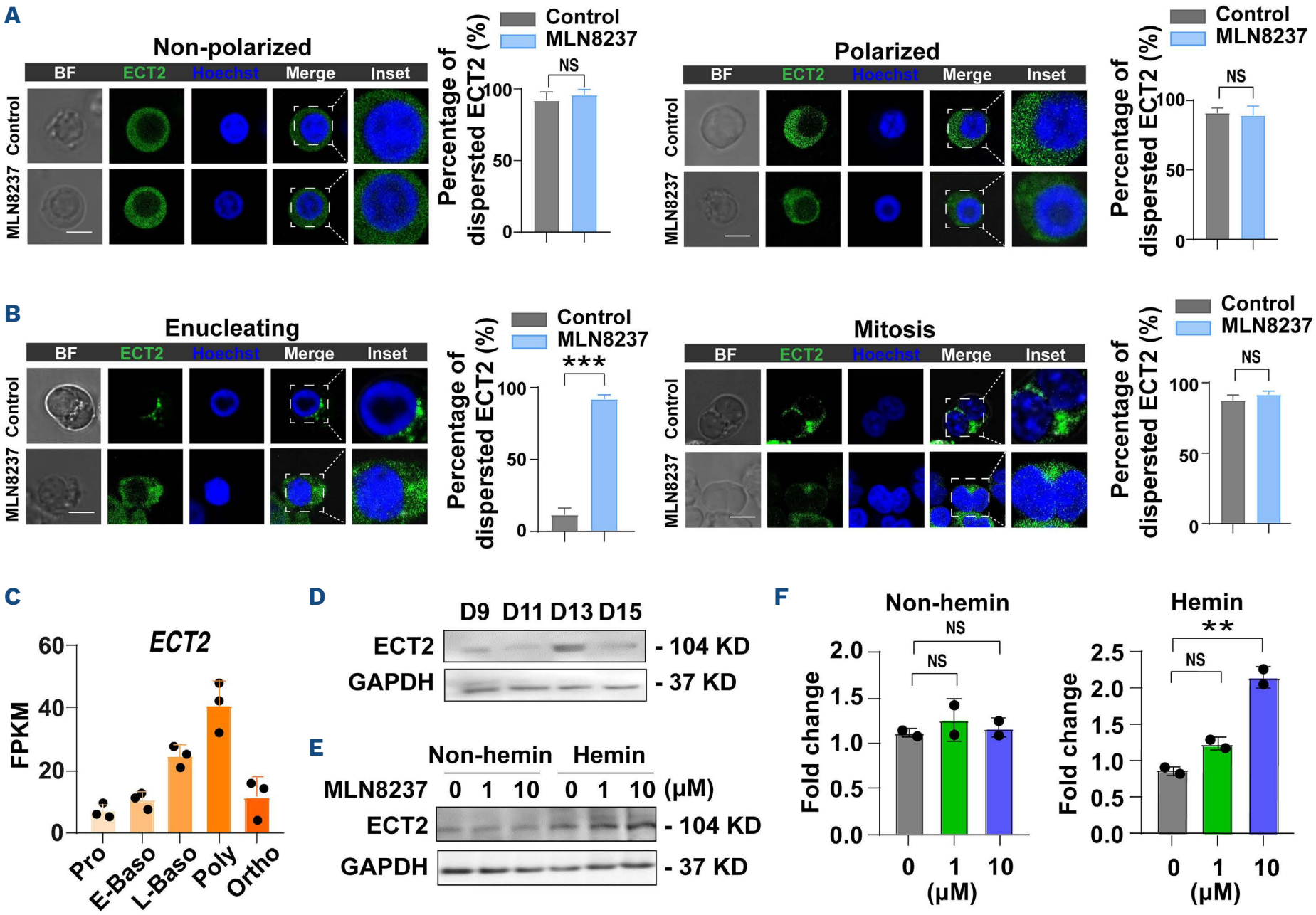

Figure 5. AURKA regulates the expression and localization of ECT2 during enucleation. (A) Confocal microscope images and statistical analysis showed cellular localization of ECT2 (epithelial cell transforming 2) in non-polarized cells and polarized cells after treatment with or without MLN8237. Scale bar =5 μm. (B) Confocal microscope images and statistical analysis showed cellular localization of ECT2 in enucleating human cells and mitotic erythroid cells after treatment with or without MLN8237. Scale bar =5 μm. (C) RNA-sequencing data of erythroblasts cultured from cord blood $CD34^+$ cells at distinct stages of development showed that the expression of *ECT2* was dramatically downregulated in orthochromatic erythroblasts (Ortho). (D) Western blotting images showed that the expression pattern of ECT2 in erythroblasts cultured for the indicated days. (E) Representative western blots showed the protein levels of ECT2 in hemin-treated or untreated K562 cells cultured with the indicated concentrations of MLN8237. (F) Quantitative analysis showed ECT2 protein levels. Pro: proerythroblasts; E-Baso: early basophilic erythroblasts; L-Baso: late basophilic erythroblasts; Poly: polychromatic erythroblasts. NS: not significant; $^{**}P<0.01$.

almost completely eliminate kinase activity.[33,34] Based on this, we generated the *AURKA* T288A allele by site-directed mutagenesis (Figure 6B) and examined the ubiquitin modification of ECT2. The results showed that the expression of *AURKA* T288A decreased ubiquitin-modified ECT2 protein in comparison to the unmutated allele (Figure 6C). In order to further confirm the relationship, we also conducted the dominant active *AURKA* T288E allele[35] and found that continuous activation of AURKA resulted in significantly enhanced ubiquitination of ECT2 (Figure 6C). These results suggest that AURKA regulates ubiquitin-mediated ECT2 degradation through direct interaction, which is, at least in part, dependent on kinase activity of AURKA.

Knockdown of ECT2 partially rescued impaired enucleation caused by AURKA inhibition

In order to more directly document that upregulation of ECT2 contributes to impaired enucleation of AURKA-deficient erythroblasts, we examined whether knockdown of ECT2 rescues the phenotypes. To this end, *ECT2* siRNA or control scramble siRNA was transfected into the erythroblasts on day 15 of culture that were simultaneously treated with MLN8237. We found that defects in enucleation caused by AURKA inhibition were rescued by knockdown of ECT2 (Figure 6D-F). In contrast to the control scramble siRNA, we validated the knockdown efficiency of *ECT2* siRNA and found that it did not alter

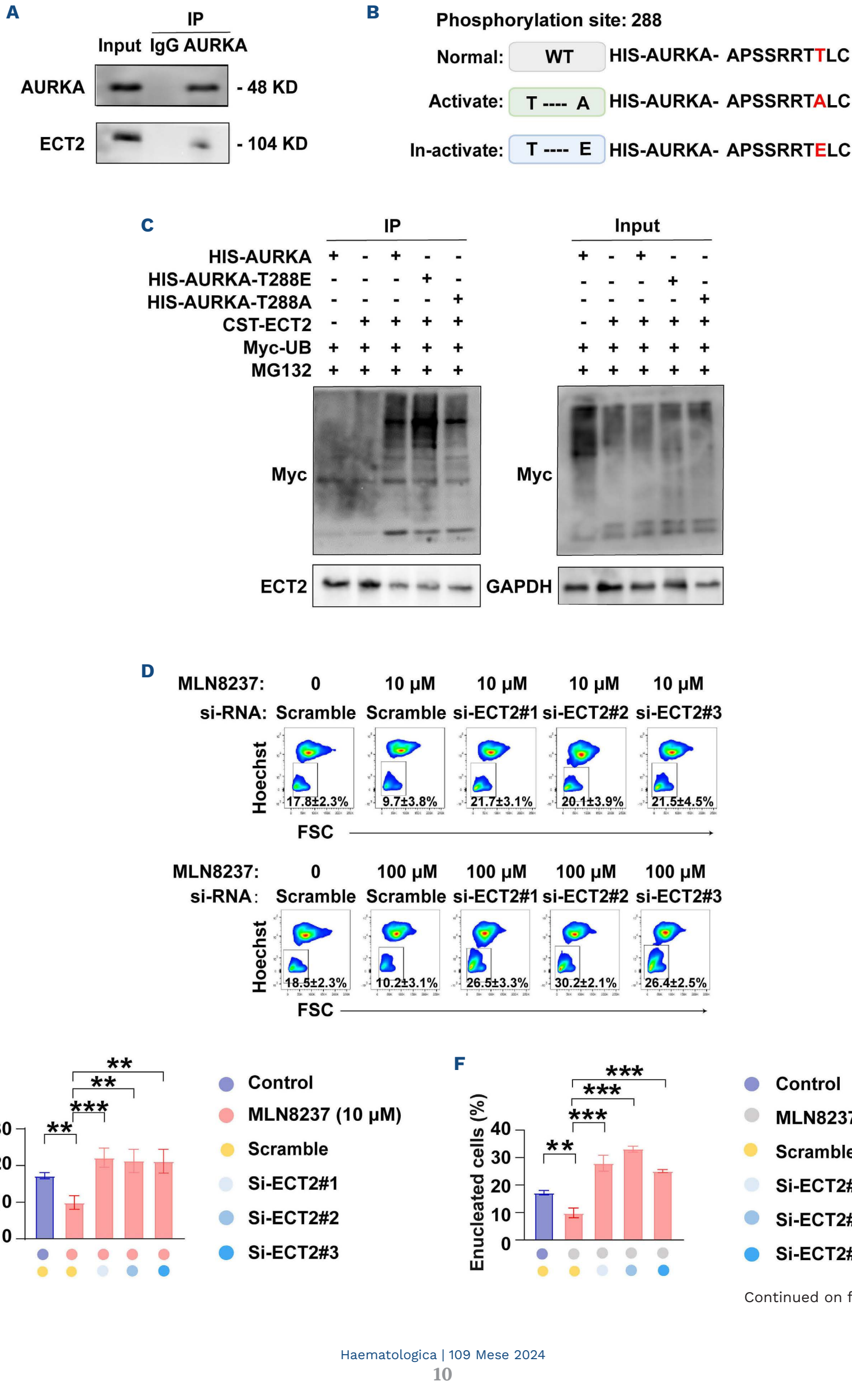

Continued on following page.

Figure 6. AURKA is responsible for ECT2 ubiquitylation and knockdown of ECT2 partially rescued impaired enucleation caused by AURKA inhibition. (A) Co-immunoprecipitation (Co-IP) showed a direct interaction between AURKA and ECT2. (B) Schematic of *AURKA* T288A and *AURKA* T288E. (C) Representative western blotting showing the ubiquitination levels in response to the exogenous expression of AURKA, ECT2, both AURKA and ECT2, as well as both *AURKA* T288A and ECT2, and both *AURKA* T288E and ECT2 in HeLa cells, respectively. (D) Representative flow cytometry profiles showed the enucleation rates of 10 μM or 100 μM MLN8237-treated erythroblasts after transfection with *ECT2* small interfing RNA (siRNA) or vehicle siRNA (Scramble) in $CD34^+$ human erythroid culture systems. (E, F) Quantitative analysis of enucleation rate of 10 μM or 100 μM MLN8237-treated erythroblasts after transfection with *ECT2* siRNA or vehicle siRNA (Scramble); ***P*<0.01, ****P*<0.001.

enucleation alone (*Online Supplementary Figure S7A, B*). However, it significantly increased the enucleation of MLN8237-treated erythroblasts (Figure 6D-F; *Online Supplementary Figure S7C, D*), indicating that the upregulation of ECT2 is responsible for the impaired enucleation following treatment with the AURKA inhibitor.

Discussion

Using pharmacological administration and genetic manipulation, we discovered that deficiency of AURKA, an aurora kinase associated with mitosis, resulted in impaired erythroblast enucleation by delaying nuclear polarization and disrupting asymmetry establishment. In practice, since enucleation has been found to be similar to cytokinesis in terms of morphological changes based on early electron microscopy, molecules involved in membrane skeletal and cytoskeletal remodeling have been broadly explored in erythroblast enucleation.[5,6,36-38] Kobayashi *et al.* investigated the effect of several microtubule-organizing centers inhibitors on cytokinesis and enucleation and showed that only EHNA, a dynein inhibitor, blocked both cytokinesis and enucleation, while monastrol (Eg5 inhibitor), ON-01910 (PLK1 inhibitor), MLN8237 (AURKA inhibitor), hesperadin (AURKB inhibitor), and LY294002 (PI3K inhibitor) just affected cytokinesis.[38] However, the conclusion is somewhat arbitrary because the effect of inhibitor concentration on protein expression is not verified. In the present study, we also performed pharmacological inhibition of AURKA kinase, but in a wider concentration range. We found that low concentrations of inhibitors indeed did not have a significant effect on enucleation, but high concentrations of inhibitors obviously inhibited enucleation. In order to confirm this, we also employed a siRNA-mediated knockdown approach in human erythroblasts and obtained consistent results. These results clarified the function of AURKA in erythroblast enucleation, which corresponds to the specific high expression of AURKA in the late stages of terminal erythroid differentiation. In our study, siRNA-mediated knockdown of AURKA more significantly impacts erythroid enucleation than the AURKA inhibitor MLN8237, due to its broader reduction of both protein presence and function. While MLN8237 specifically targets phosphorylation without altering overall protein levels, leading to a less substantial effect. Higher concentrations significantly inhibit enucleation, revealing a direct correlation between the extent of AURKA inhibition and its impact on enucleation. In addition, it also reflects the different expression levels or activity that may be required for the same regulator to function in cytokinesis and enucleation.

Nuclear polarization is generally considered to be the initial step towards erythroblast enucleation and appears to be important for successful enucleation. Microtubules are now thought to be required for nuclear polarization.[5] During enucleation, microtubules form a cage-like structure surrounding the nucleus and the nucleus is ultimately released from the microtubule cage.[5,39] In the present study, we found that inhibition of AURKA, impaired nuclear polarization. Of note, AURKA deficiency had no effect in microtubule organization in enucleating erythroblasts, while it results in disordered microtubule organization in mitosis of erythroid cells, suggesting that the polarization disorder in enucleation caused by AURKA deficiency is microtubule-independent. During embryonic development, the function of AURKA for establishment of cell polarity is also independent of its role in microtubule nucleation.[40] We also determined that AURKA deficiency caused disturbance of centrosome formation, and inhibition of centrosome formation resulted in polarization damage, consistent with previous reports that centrosome loss during erythroid differentiation causes tetraploidy and impairs enucleation through testing CDK5RAP2- and centrosome-deficient erythroblasts.[25] In recent years, increasing findings reveal that the centrosome provides signals that induce cell polarization during embryonic development, which is independent of function as the microtubule-organizing center.[41,42] Centrosome appears to provide a “beacon” for guiding the spherical erythroblast to select or confirm the orientation of nuclear polarization before microtubule organization.

A recent finding from a study by Nowak *et al.* shows that F-actin forms a contractile ring merely at the completion of enucleation to help finally separate the pyrenocyte from the reticulocyte,[43] suggesting that the contractile ring is unlikely to carry out the nuclear protrusion during enucleation. Our present data show that immediately after nuclear polarization, AURKA migrates to the anterior end of the protrusive nucleus to alter the protein distribution of ECT2. Of note, the ECT2 distribution change regulated by AURKA is not exist during cytokinesis. ECT2 encodes a potential guanine nucleotide-exchange factor that catalyzes the exchange of GDP for GTP for Rho GTPases.[44]

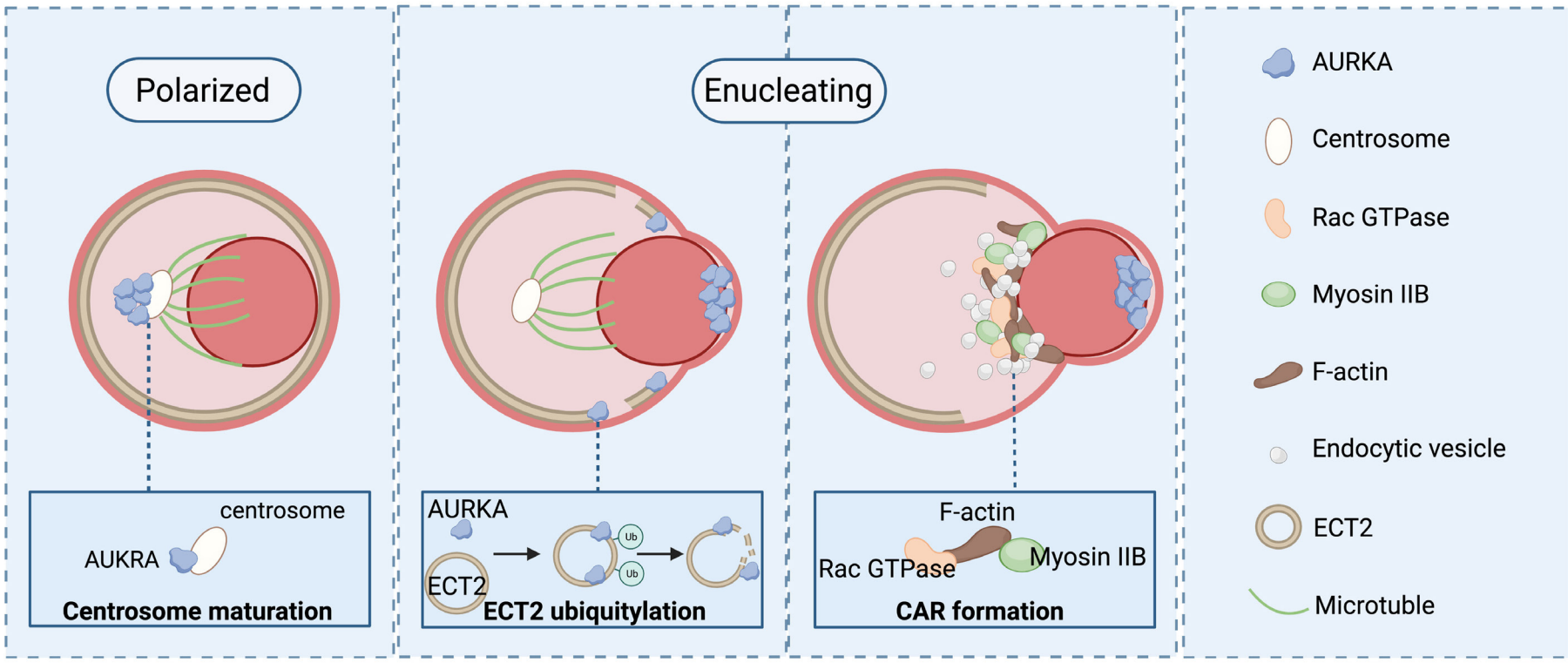

Figure 7. A new model for erythroblast enucleation. Schematic of enucleation: first, AURKA regulates centrosome maturation and localization to provide orientation for the cell nucleus. Then, AURKA translocates to the anterior end of the protrusive nucleus to directly degrade ECT2 to form asymmetric contractility, providing force for expelling the nucleus during enucleation. Under the control of Rac GTPases, F-actin, interacting with myosin IIB, polymerizes to form a narrow contractile ring in the cleavage furrow to complete the final separation of the pyrenocyte from the reticulocyte. During this transfer, endocytic vesicles move and fuse at the division plane to provide the extra plasma membranes.

Rho GTPases have been shown to play important roles in erythroblast enucleation by regulating cytoskeletal rearrangements and other physiological activities.[8,26,27] During embryonic development in *C. elegans*, ECT2 is uniformly distributed at the cortex prior to cell polarity formation, but was excluded from the posterior cortex at the onset of symmetry breaking,[28] revealing the crucial role of ECT2 in controlling contractile asymmetry. Notably, another report showed that AIR-1 (Aurora A kinase in *C. elegans*) depletion influences ECT2 cortical localization, resulting in appearance of multiple PAR-2 polarity axis due to pronounced cortical contractions on the embryo surface.[40] After nuclear polarization, ECT2 needs to exclude from anterior end of polarity axis and form asymmetric contractility to provide force for expelling the nucleus during enucleation. The asymmetric contractility contributed by the asymmetrical distribution of ECT continues to provide expulsion force until F-actin forms a narrow contractile ring to complete the final separation of the pyrenocyte from the reticulocyte. Although the effect of AURKA on the localization of ECT2 has been reported,[40] the mechanism by which AURKA regulates ECT2 to establish cellular asymmetry remains unclear. We showed that the altered distribution of ECT2 was accompanied by migration of AURKA to the anterior end of the protrusive nucleus, and that the expression levels of AURKA and ECT2 were opposite. Coupled with the fact that direct interaction is proved by co-IP analysis, we speculate that AURKA may directly degrade ECT2. As a serine/threonine protein kinase, AURKA mainly acts by phosphorylation of several substrates that are involved in cell cycle regulation and mitosis progression. In addition to phosphorylation activity, AURKA has been predicted to possess ubiquitination activity and acts as a potential ubiquitinating enzyme.[31,32] We found that overexpression of AURKA promoted ubiquitination of ECT2. Of note, site-specific mutation experiment demonstrated that the ubiquitination function of AURKA on ECT2 is dependent on kinase activity. Previous studies display that AURKA regulates MYC and METTL14 expression by inhibiting their ubiquitylation and degradation in a kinase-independent manner in breast cancer stem-like cells.[45,46] The complex and inconsistent observations implies that AURKA may function in different cell types through different activities or in different ways. In summary, our study describes a specific and novel temporal and spatial localization of AURKA and demonstrates that AURKA interacts with γ-tubulin and ECT2 to control centrosome localization and ECT2 degradation, contributing to nuclear polarization and expulsion. These findings further advance our understanding of erythroblast enucleation and provide new insights into associated mechanisms. A new model for erythroblast enucleation is proposed as follows (Figure 7). After exiting the cell cycle, spherical orthochromatic erythroblast used the centrosome, regulated by AURKA as a “beacon” to determine the direction of polarization, and then the condensed nucleus moves to one side of the cell under the action of the unipolar spindle formed by microtubules. Subsequently, AURKA translocates to the anterior end of the protrusive nucleus and directly degrade ECT2 to form asymmetric contractility, providing force for expelling the nucleus during enucleation. Under

the control of Rac GTPases, F-actin, interacting with myosin IIB, polymerizes to form a narrow contractile ring in the cleavage furrow to complete the final separation of the pyrenocyte from the reticulocyte. During this transfer, endocytic vesicles move and fuse at the division plane to provide the extra plasma membranes.

Contributions

YX, PJ and YL designed experiments, performed research, analyzed the data and drafted materials and methods. HZ, WL, YZ, YL, JC, TZ, YW and YL performed research. XA and JZ analyzed the data and edited the manuscript. SZ conceived the subject, designed experiments, analyzed data and wrote the manuscript.

Disclosures

No conflicts of interest to disclose.

Funding

This work was supported by National Natural Science Foundation of China (Nos. 82270124, 81870095 and 82370125); Program for Science and Technology Innovation Talents in Universities of Henan Province (No. 23HASTIT040); Science and Technology Development Program of Henan Province (Nos. 232300421056 and 232102311141); Young Backbone Teacher Training program in Universities of Henan Province (No. 2021GGJS013) and Scientific Programs of Zhengzhou University (No. 2022RC0329020401231).

Data-sharing statement

Data and materials supporting the findings are available from the corresponding authors upon request. All other relevant data supporting the key findings of this study are available within the article and its Online Supplementary Appendix.

References

1. Hu J, Liu J, Xue F, et al. Isolation and functional characterization of human erythroblasts at distinct stages: implications for understanding of normal and disordered erythropoiesis in vivo. Blood. 2013;121(16):3246-3253.
2. Popova EY, Krauss SW, Short SA, et al. Chromatin condensation in terminally differentiating mouse erythroblasts does not involve special architectural proteins but depends on histone deacetylation. Chromosome Res. 2009;17(1):47-64.
3. Li X, Mei Y, Yan B, et al. Histone deacetylase 6 regulates cytokinesis and erythrocyte enucleation through deacetylation of formin protein mDia2. Haematologica. 2017;102(6):984-994.
4. Ji P, Yeh V, Ramirez T, Murata-Hori M, Lodish HF. Histone deacetylase 2 is required for chromatin condensation and subsequent enucleation of cultured mouse fetal erythroblasts. Haematologica. 2010;95(12):2013-2021.
5. Wang J, Ramirez T, Ji P, Jayapal SR, Lodish HF, Murata-Hori M. Mammalian erythroblast enucleation requires PI3K-dependent cell polarization. J Cell Sci. 2012;125(Pt 2):340-349.
6. Ubukawa K, Guo YM, Takahashi M, et al. Enucleation of human erythroblasts involves non-muscle myosin IIB. Blood. 2012;119(4):1036-1044.
7. Konstantinidis DG, Pushkaran S, Johnson JF, et al. Signaling and cytoskeletal requirements in erythroblast enucleation. Blood. 2012;119(25):6118-6127.
8. Ji P, Jayapal SR, Lodish HF. Enucleation of cultured mouse fetal erythroblasts requires Rac GTPases and mDia2. Nat Cell Biol. 2008;10(3):314-321.
9. Keerthivasan G, Small S, Liu H, Wickrema A, Crispino JD. Vesicle trafficking plays a novel role in erythroblast enucleation. Blood. 2010;116(17):3331-3340.
10. An C, Huang Y, Li M, et al. Vesicular formation regulated by ERK/MAPK pathway mediates human erythroblast enucleation. Blood Adv. 2021;5(22):4648-4661.
11. Willems E, Dedobbeleer M, Digregorio M, Lombard A, Lumapat PN, Rogister B. The functional diversity of Aurora kinases: a comprehensive review. Cell Div. 2018;13:7.
12. Joukov V, De Nicolo A. Aurora-PLK1 cascades as key signaling modules in the regulation of mitosis. Sci Signal. 2018;11(543):eaar4195.
13. Carmena M, Wheelock M, Funabiki H, Earnshaw WC. The chromosomal passenger complex (CPC): from easy rider to the godfather of mitosis. Nat Rev Mol Cell Biol. 2012;13(12):789-803.
14. Carmena M, Earnshaw WC. The cellular geography of aurora kinases. Nat Rev Mol Cell Biol. 2003;4(11):842-854.
15. Marumoto T, Honda S, Hara T, et al. Aurora-A kinase maintains the fidelity of early and late mitotic events in HeLa cells. J Biol Chem. 2003;278(51):51786-51795.
16. Cowley DO, Rivera-Pérez JA, Schliekelman M, et al. Aurora-A kinase is essential for bipolar spindle formation and early development. Mol Cell Biol. 2009;29(4):1059-1071.
17. Sessa F, Mapelli M, Ciferri C, et al. Mechanism of Aurora B activation by INCENP and inhibition by hesperadin. Mol Cell. 2005;18(3):379-391.
18. Portella G, Passaro C, Chieffi P. Aurora B: a new prognostic marker and therapeutic target in cancer. Curr Med Chem. 2011;18(4):482-496.
19. Regan JL, Sourisseau T, Soady K, et al. Aurora A kinase regulates mammary epithelial cell fate by determining mitotic spindle orientation in a Notch-dependent manner. Cell Rep. 2013;4(1):110-123.
20. An X, Schulz VP, Li J, et al. Global transcriptome analyses of human and murine terminal erythroid differentiation. Blood. 2014;123(22):3466-3477.
21. Mei Y, Liu Y, Ji P. Understanding terminal erythropoiesis: An update on chromatin condensation, enucleation, and reticulocyte maturation. Blood Rev. 2021;46:100740.
22. Rutherford TR, Clegg JB, Weatherall DJ. K562 human leukaemic cells synthesise embryonic haemoglobin in response to haemin. Nature. 1979;280(5718):164-165.
23. Rutherford T, Clegg JB, Higgs DR, Jones RW, Thompson J, Weatherall DJ. Embryonic erythroid differentiation in the human leukemic cell line K562. Proc Natl Acad Sci U S A. 1981;78(1):348-352.
24. Wong YL, Anzola JV, Davis RL, et al. Cell biology. Reversible centriole depletion with an inhibitor of Polo-like kinase 4. Science. 2015;348(6239):1155-1160.
25. Tátrai P, Gergely F. Centrosome function is critical during terminal erythroid differentiation. EMBO J. 2022;41(14):e108739.

26. Ubukawa K, Goto T, Asanuma K, et al. Cdc42 regulates cell polarization and contractile actomyosin rings during terminal differentiation of human erythroblasts. Sci Rep. 2020;10(1):11806.
27. Kalfa TA, Zheng Y. Rho GTPases in erythroid maturation. Curr Opin Hematol. 2014;21(3):165-171.
28. Motegi F, Sugimoto A. Sequential functioning of the ECT-2 RhoGEF, RHO-1 and CDC-42 establishes cell polarity in Caenorhabditis elegans embryos. Nat Cell Biol. 2006;8(9):978-985.
29. Liot C, Seguin L, Siret A, Crouin C, Schmidt S, Bertoglio J. APCcdh1 mediates degradation of the oncogenic Rho-GEF Ect2 after mitosis. PloS One. 2011;6(8):e23676.
30. Reiter LT, Seagroves TN, Bowers M, Bier E. Expression of the Rho-GEF Pbl/ECT2 is regulated by the UBE3A E3 ubiquitin ligase. Hum Mol Genet. 2006;15(18):2825-2835.
31. Yang C, You D, Huang J, Yang B, Huang X, Ni J. Effects of AURKA-mediated degradation of SOD2 on mitochondrial dysfunction and cartilage homeostasis in osteoarthritis. J Cell Physiol. 2019;234(10):17727-17738.
32. Wang X, Li Y, He M, et al. UbiBrowser 2.0: a comprehensive resource for proteome-wide known and predicted ubiquitin ligase/deubiquitinase-substrate interactions in eukaryotic species. Nucleic Acids Res. 2022;50(D1):D719-D728.
33. Ohashi S, Sakashita G, Ban R, et al. Phospho-regulation of human protein kinase Aurora-A: analysis using anti-phospho-Thr288 monoclonal antibodies. Oncogene. 2006;25(59):7691-7702.
34. Littlepage LE, Wu H, Andresson T, Deanehan JK, Amundadottir LT, Ruderman JV. Identification of phosphorylated residues that affect the activity of the mitotic kinase Aurora-A. Proc Natl Acad Sci U S A. 2002;99(24):15440-15445.
35. Huang W, She L, Chang XY, et al. Protein kinase LKB1 regulates polarized dendrite formation of adult hippocampal newborn neurons. Proc Natl Acad Sci U S A. 2014;111(1):469-474.
36. Keerthivasan G, Liu H, Gump JM, Dowdy SF, Wickrema A, Crispino JD. A novel role for survivin in erythroblast enucleation. Haematologica. 2012;97(10):1471-1479.
37. Koury ST, Koury MJ, Bondurant MC. Cytoskeletal distribution and function during the maturation and enucleation of mammalian erythroblasts. J Cell Biol. 1989;109(6 Pt 1):3005-3013.
38. Kobayashi I, Ubukawa K, Sugawara K, et al. Erythroblast enucleation is a dynein-dependent process. Exp Hematol. 2016;44(4):247-256.
39. Thom CS, Traxler EA, Khandros E, et al. Trim58 degrades Dynein and regulates terminal erythropoiesis. Dev Cell. 2014;30(6):688-700.
40. Kapoor S, Kotak S. Centrosome Aurora A regulates RhoGEF ECT-2 localisation and ensures a single PAR-2 polarity axis in C. elegans embryos. Development. 2019;146(22):dev174565.
41. Feldman JL, Priess JR. A role for the centrosome and PAR-3 in the hand-off of MTOC function during epithelial polarization. Curr Biol. 2012;22(7):575-582.
42. Bienkowska D, Cowan CR. Centrosomes can initiate a polarity axis from any position within one-cell C. elegans embryos. Curr Biol. 2012;22(7):583-589.
43. Nowak RB, Papoin J, Gokhin DS, et al. Tropomodulin 1 controls erythroblast enucleation via regulation of F-actin in the enucleosome. Blood. 2017;130(9):1144-1155.
44. Miki T, Smith CL, Long JE, Eva A, Fleming TP. Oncogene ect2 is related to regulators of small GTP-binding proteins. Nature. 1993;362(6419):462-465.
45. Zheng F, Yue C, Li G, et al. Nuclear AURKA acquires kinase-independent transactivating function to enhance breast cancer stem cell phenotype. Nat Commun. 2016;7:10180.
46. Peng F, Xu J, Cui B, et al. Oncogenic AURKA-enhanced N(6)-methyladenosine modification increases DROSHA mRNA stability to transactivate STC1 in breast cancer stem-like cells. Cell Res. 2021;31(3):345-361.

Supplementary methods

Ubiquitylation assay. Cells were transfected with plasmids expressing Myc-Ub for 48 h, with or without His-AURKA and/or GST-ECT2 vectors. Cells were collected and washed in cold PBS after treated with MG132 (Sigma-Aldrich) for 6 h and then lysed in RIPA lysis buffer (Cowin Biotechnology) containing phosphatase inhibitors and protease inhibitor. Cell lysates were incubated with magnetic protein A/G beads (Bio-Rad) for 2 hours, followed by immunoprecipitation using anti-AURKA antibody for 12 hours at 4°C and subsequent washing. The immunoprecipitation mixture was boiled in the SDS sample buffer, separated by 10% SDS-PAGE, transferred onto a nitrocellulose membrane (Bio-Rad), and subjected to Western blotting procedures.

Overexpression of ECT2 in $CD34^+$ Cells. The ECT2 gene was cloned into the pLVX-puro lentiviral vector. The ECT2 coding sequence was inserted into the pLVX-puro vector backbone through standard molecular cloning techniques, and the integrity of the construct was confirmed by DNA sequencing. Human $CD34^+$ hematopoietic stem cells were transduced with the recombinant pLVX-puro-ECT2 lentivirus. Following transduction, the cells were selected with puromycin for 3 days to enrich for populations expressing ECT2. The overexpression of ECT2 was confirmed by quantitative PCR to ensure efficient transduction and expression within the cells.

Imaging flow cytometry. Terminal erythroid cells differentiated from $CD34^+$ cells were fixed and then stained with antibodies specific for AURKA and ECT2. After staining, the cells were analyzed using an Image Stream X Mark II (ISX-100, Amnis/Luminex), and the images were subsequently analyzed using the IDEAS software (Amnis).

Supplementary Figure Legends

Supplemental Figure 1. Efficient AURKA knockdown impacts erythroblast enucleation and nuclear polarization.

(A) Schematic diagram of enucleation in human $CD34^+$ cells followed by erythroid cell culture. (B) Flow cytometry gating strategy was utilized for enucleation of sorted mouse bone marrow orthochromatic erythroblasts, followed by an 18 hours culture period. (C) Enucleation was assessed in the presence or absence of MLN8237 for sorted mouse orthochromatic erythroblasts for 18 hours. (D) Model of a

siRNA-mediated knockdown approach in human erythroblasts. (E) Effective downregulation of AURKA in human erythroblasts confirmed by western blot analysis following treatment with three distinct AURKA siRNA oligonucleotides and scramble siRNA. (F) Quantitative analysis showing nuclear and cellular dimensions in MLN8237-treated and control erythroblasts. (G) Representative cytospin images displaying the extent of enucleation in erythroblasts treated with AURKA-specific siRNA and control. Scale bar = 10 μm. (H) Quantitative assessment of the mean Δ centroid in erythroblasts treated with AURKA-specific siRNA and control.

Supplemental Figure 2. Dynamic changes in AURKA localization during erythroblast enucleation in mice.

Confocal microscopy images capturing AURKA distribution (red) through different stages of erythroblast enucleation in mouse cells. Ter119 antibody, marking the erythroid cell membrane, and Hoechst33342, staining the nucleus, are used to delineate cellular components. Scale bar=5 μm.

Supplemental Figure 3. Effect of AURKA-specific siRNAs on the location of AURKA and γ-tubulin during erythroblast enucleation.

(A) Co-immunoprecipitation (co-IP) showed a direct interaction between AURKA and γ-tubulin. (B) Representative Western blots showed the protein levels of γ-tubulin in hemin-treated or untreated K562 cells cultured with indicated concentrations of MLN8237. (C) Quantitative analysis showed γ-tubulin protein levels. Confocal microscope images showed the colocalization of AURKA and γ-tubulin in non-polarized cells (D), polarized cells (E) and enucleating cells (F) treated with AURKA-specific siRNA. Scale bar=5 μm.

Supplemental Figure 4. Dynamic interaction between AURKA and ECT2 during erythroblast enucleation, observed through Image Stream analysis.

This series of high-resolution images captures the evolving relationship between AURKA and ECT2 in polarization (A) and enucleting (B) stages of erythroblast through image stream analysis. Scale bar=7 μm. (C) Quantitative analysis of the distance of AURKA foci to the center of cytoplasm. (D) Quantitative analysis of the distance of the center of ECT2 fluorescence to the center of nucleus.

Supplemental Figure 5. Impact of AURKA inhibition on ECT2 translocation in mice bone marrow erythroblasts.

Confocal microscope images showed cellular localization of ECT2 in non-polarized cells (A), polarized cells (B) and enucleating cells (C) after treatment with or without MLN8237 in mice bone marrow erythroblasts. Scale bar=5 μm.

Supplemental Figure 6. Effects of ECT2 over-expression on erythroblast differentiation and enucleation.

(A) PCR analysis confirming significant up-regulation of ECT2 expression in $CD34^+$ cells following transfection with ECT2 over-expression vectors, establishing effective gene manipulation. (B-C) Analysis of erythroid differentiation in cells over-expressing ECT2, showing minimal changes compared to control groups. (D-F) Quantitative and qualitative assessments of enucleation in erythroblasts with elevated ECT2 levels.

Supplemental Figure 7. ECT2 knockdown mitigates enucleation deficits in AURKA-inhibited erythroblasts.

(A) PCR analysis confirmed significant downregulation of ECT2 expression after treatment with three distinct siRNA oligonucleotides. (B) Examination of erythroblast enucleation following transfection with ECT2-specific siRNA and control. (C-D) Representative cytospin images displaying erythroblast enucleation in cells co-treated with MLN8237 (10 μM or 100 μM) and ECT2-specific siRNA. Scale bar = 10 μm.

Figure S1

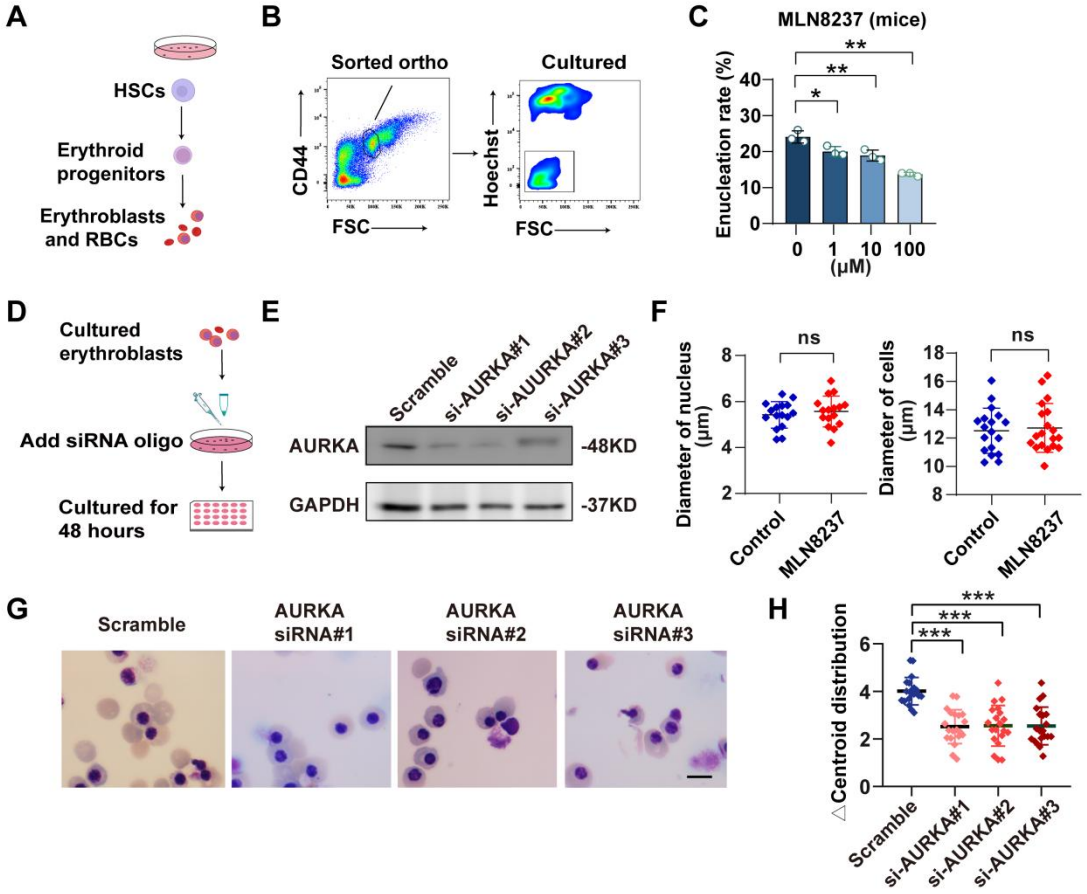

Supplemental Figure 1. Efficient AURKA knockdown impacts erythroblast enucleation and nuclear polarization.

Figure S2

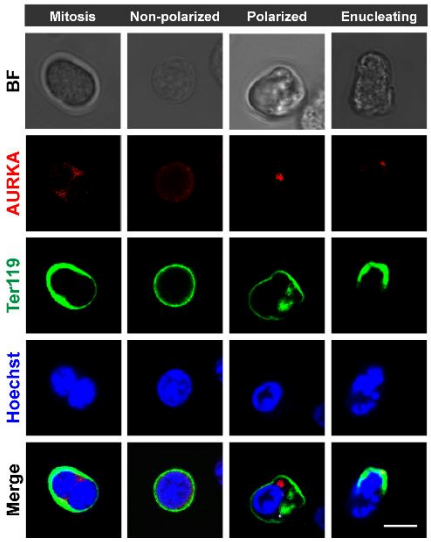

Supplemental Figure 2. Dynamic changes in AURKA localization during

erythroblast enucleation in mice.

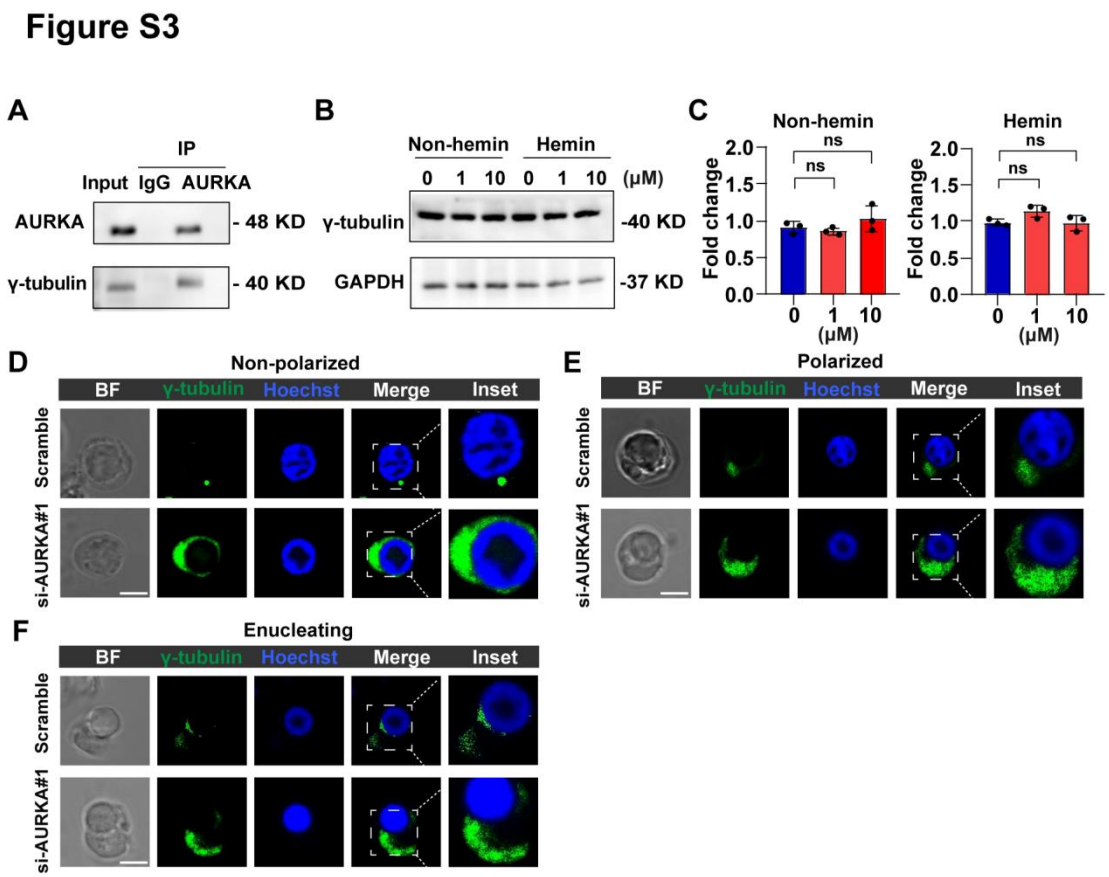

Supplemental Figure 3. Effect of AURKA-specific siRNAs on the location of γ-tubulin during erythroblast enucleation.

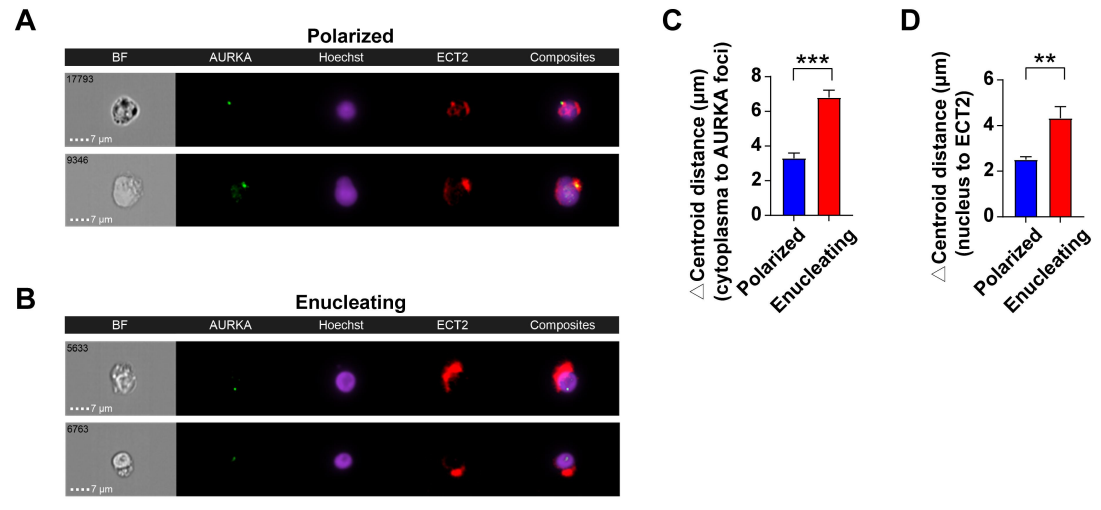

Supplemental Figure 4. Dynamic interaction between AURKA and ECT2 during

erythroblast enucleation, observed through Image Stream analysis.

Figure S5

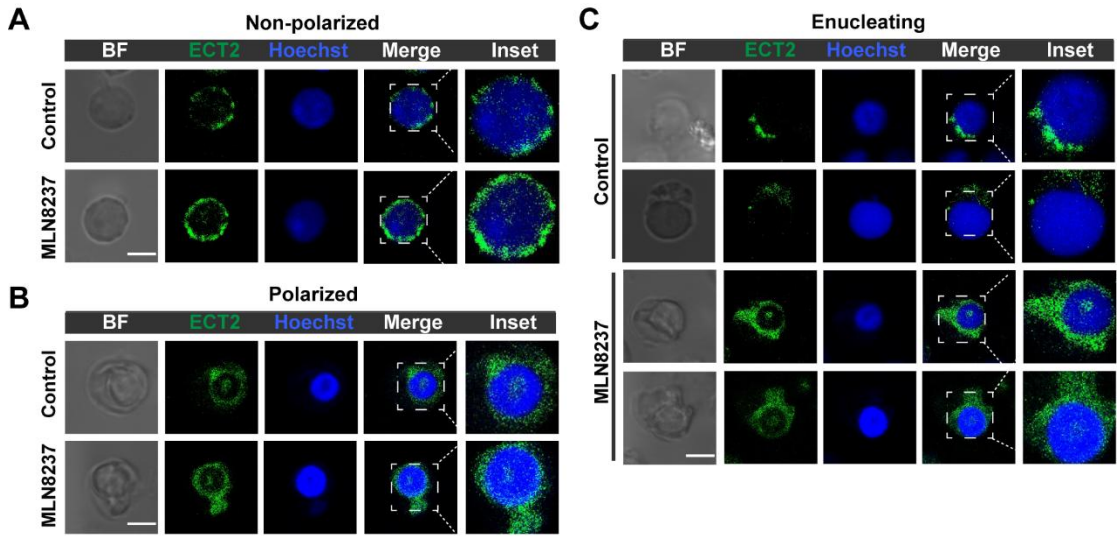

Supplemental Figure 5. Impact of AURKA inhibition on ECT2 translocation in mice bone marrow erythroblasts.

Figure S6

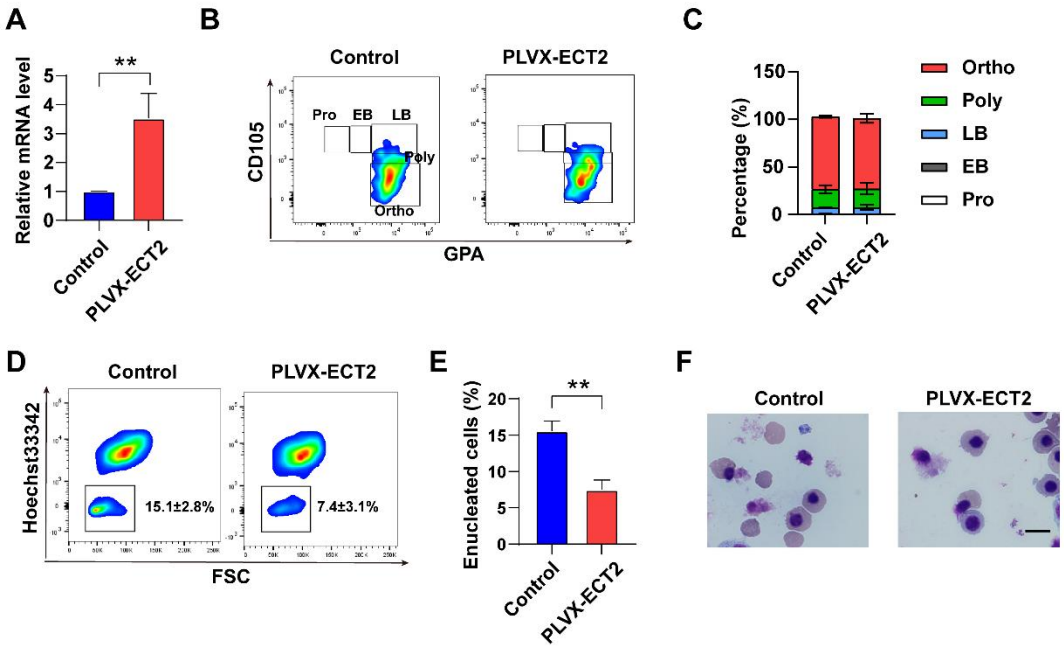

Supplemental Figure 6. Effects of ECT2 overexpression on erythroblast differentiation and enucleation.

Figure S7

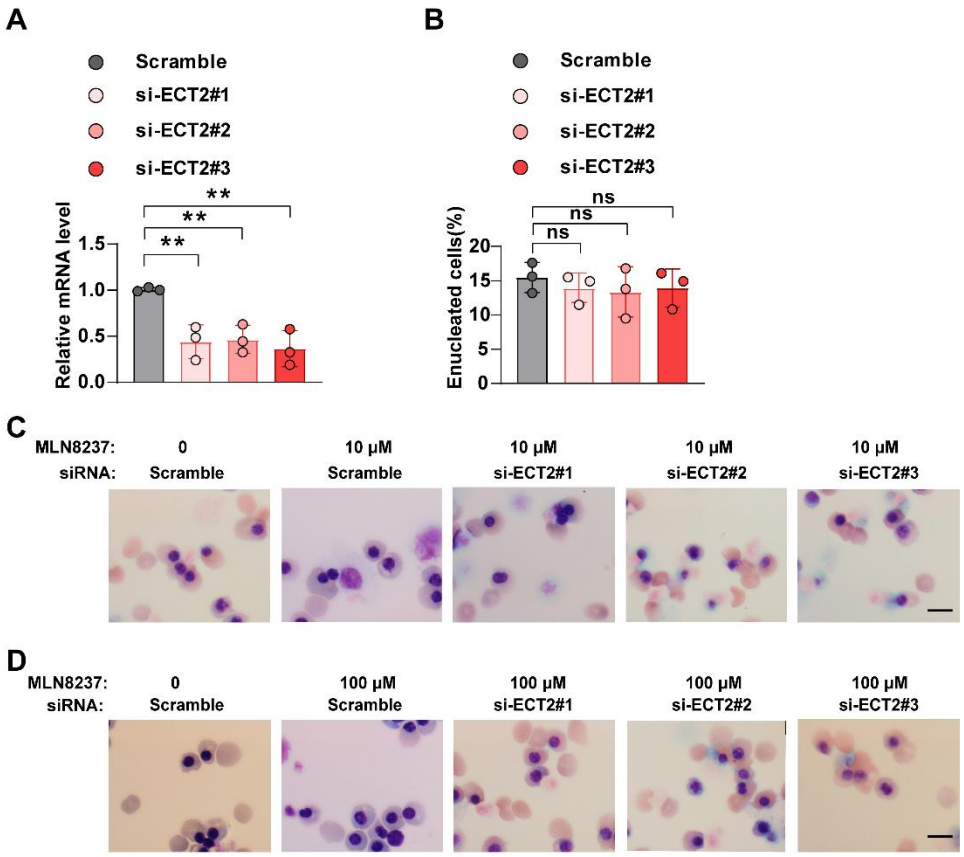

Supplemental Figure 7. ECT2 knockdown mitigates enucleation deficits in AURKA-inhibited erythroblasts.

Supplemental Table 1. Antibodies for Western blotting and immunofluorescence

Antibodies	Antibodies	working concentration	company
AURKA	Rabbit monoclonal antibody	1：1000	Cell Signaling Technology
AURKB	Rabbit monoclonal antibody	1：1000	Cell Signaling Technology
Anti-gamma Tubulin	Rabbit monoclonal antibody	1：1000	Abcam
ECT2	Murine monoclonal antibody	1：1000	Santa Cruz Biotechnology
GAPDH	Murine monoclonal antibody	1：1000	Proteintech
Goat Anti Rabbit	-	1：2000	Proteintech
Goat Anti Mouse	-	1：2000	Proteintech
AURKB	Rabbit monoclonal antibody	1：100	Cell Signaling Technology
AURKB	Rabbit monoclonal antibody	1：100	Cell Signaling Technology
AURKA	Rabbit monoclonal antibody	1：100	Signalway Antibody
ECT2	Murine monoclonal antibody	1：100	Santa Cruz Biotechnology
Hochest33342	-	1：100	Solarbio
Mouse Anti-γ Tubulin antibody	Murine monoclonal antibody	1：100	Bioss
Actin-Tracker Green	-	1：100	Beyotine
Goat Anti Mice FITC	-	1：100	Solarbio
Goat Anti Rabbit RBITC	-	1：100	Bioss

Supplemental Table 2. qRT-PCR primers

Gene	Primer
AURKA：	Forward：GAGGTCCAAAACGTGTTCTCG
	Reverse：ACAGGATGAGGTACACTGGTTG
AURKB：	Forward：CAGTGGGACACCCGACATC
	Reverse：GTACACGTTTCCAAACTTGCC
TUBG1：	Forward：AGCTGGTGTCTACCATCATGT
	Reverse：CGTAGTGAGAGGGGTGTAGC
ECT2：	Forward：ACTACTGGGAGGACTAGCTTG
	Reverse：CACTCTTGTTTCAATCTGAGGCA

Supplemental Table 3. The siRNA sequences and overexpression primers

Primer name：	Primer sequence：
ECT2-siRNA (#1)	forward primer：GCGGGUUGAAACAAUUUCUTT
	Reverse primer：AGAAAUUGUUUCAACCCGCTT
ECT2-siRNA (#2)	forward primer：GACCACCAGUUGUAUUAAATT
	Reverse primer：UUUAAUACAACUGGUGGUCTT
ECT2-siRNA (#3)	forward primer：GAAGCCAGAAUGGAUUUAUTT
	Reverse primer：AUAAAUCCAUUCUGGCUUCTT
AURKA-siRNA (#1)	forward primer：GCCGGUUCAGAAUCAGAAGTT
	Reverse primer：CUUCUGAUUCUGAACCGGCTT
AURKA-siRNA (#2)	forward primer：GGCUCUUAAAGUGUUAUUUTT
	Reverse primer：AAAUAACACUUUAAGAGCCTT
AURKA-siRNA (#3)	forward primer：GCAAUUUCCUUGUCAGAAUTT
	Reverse primer：AUUCUGACAAGGAAAUUGCTT
ECT2-overexpress -plvx	forward primer：GGATCTTCCAGAGATGGATCCATGGCTGAAAATA GTGTATTAACATCC
	Reverse primer：CTGCCGTTCGACGATCTCGAGTCATATCAAATGA GTTGTAGATCTACTTAACG